Kilowatt-class high energy frequency conversion to 95 J at 10 Hz at 515 nm

Martin Divoky[1], Jonathan Phillips[2], Jan Pilar[1], Martin Hanus[1], Petr Navratil[1], Ondrej Denk[1], Tomas Paliesek[1], Patricie Severova[1], Danielle Clarke[2], Martin Smrz[1], Thomas Butcher[2], Chris Edwards[2], John Collier[2] and Tomas Mocek[1]

[1] *HiLASE Centre, Institute of Physics of the Czech Academy of Sciences, Za Radnici 828, 25241, Dolni Brezany, Czech Republic*

[2] *Central Laser Facility, STFC Rutherford Appleton Laboratory, Didcot, OX11 0QX, UK*

Abstract We report on frequency doubling of high energy, high repetition rate ns pulses from a cryogenically gas cooled multi-slab Yb:YAG laser system Bivoj/DiPOLE, using a type-I phase matched LBO crystal. We achieved conversion to 515 nm with energy of 95 J at repetition rate of 10 Hz and conversion efficiency of 79%. High conversion efficiency was achieved due to successful depolarization compensation of the fundamental input beam.

Key words: diode pumped solid state laser, frequency conversion, high energy, high average power

I. INTRODUCTION

10.1017/hpl.2023.60

Frequency conversion of high energy, high average power (HE-HAP) diode pumped laser systems opens new applications from underwater laser shock peening of complex samples[1], laser induced damage testing at broader wavelength ranges to pumping of Ti:sapphire and optical parametric chirped pulse amplification (OPCPA) systems[2-4]. Recently, the HE-HAP frequency conversion gained even more importance due to the success of inertial confinement fusion experiments[5].

Currently many laser systems with second harmonic conversion operate at, or above, kilowatt average power, but only with low pulse energy of a few mJ[6] or J[7]. The highest energy achieved around wavelength of 500 nm on high average power system before this work was 60 J[8].

In this paper we report second harmonic generation of 95 J at repetition rate of 10 Hz from laser system Bivoj/DiPOLE [9,10], which corresponds to 950 W of average power. It is, to the best of our knowledge, the highest average power in a high energy system with energy >1 J with wavelength around 500 nm and corresponds to 58% increase to the state-of-the-art. Conversion efficiency of 79% was achieved by using flat top beam and pulse profiles and by successful optimization of depolarization by polarimetric method[11].

II. EXPERIMENT

The output from a high average power Yb:YAG laser system Bivoj/DiPOLE at 1030 nm was frequency converted to 515 nm using type I phase matching in a lithium triborate (LBO) crystal. The LBO crystal (Coherent Inc.) was optimized for second harmonic generation (SHG) from 1030 nm laser radiation. The crystal had an aperture of 60 × 60 mm^2, thickness of 13 mm and cut angles theta of 90° and phi of 13.6°. Dual band anti-reflection (AR) coatings for 1030 nm and 515 nm were used on both faces to minimize total transmission losses to 0.25% and 0.75%,

https://doi.org/10.1017/hpl.2023.60 Published online by Cambridge University Press

respectively. The crystal was placed into the windowless oven (IB Photonics) for temperature stabilization. The temperature was set to 30°C. Higher temperatures provided better conversion stability, as it uses ambient air to cool down the crystal, but lower conversion efficiency, because large difference between ambient temperature and the oven temperature creates higher temperature gradients in the crystal. Laser beam from laser system is propagated to harmonic conversion setup through series of telescopes. They de-magnify the laser beam 1.56 times from 77 × 77 mm^2 to 49 × 49 mm^2 to increase the energy fluence on the crystal. Layout of the harmonic conversion setup can be seen in Figure 1. A pair of zero order waveplates (λ/2, λ/4) was used to adjust polarization at the input of the crystal to improve the conversion efficiency by maximizing the energy in the polarization parallel with the principal plane of the crystal. After passing through the crystal, the high-power beam containing unconverted fundamental and converted second harmonic beam was terminated in the water-cooled absorption beam dump. The 1030 nm light was absorbed in water and the 515 nm light was absorbed in colored glass filters suspended in the water tank. Glass plates with different absorption bands were used to distribute the energy absorption equally among them. In front of the beam dump a sampling wedge (dielectrically coated R~1% at 1030 nm and 515 nm) was placed so that a low power reflection could be acquired and used for diagnostics. The diagnostic beam was divided according to wavelength by a dichroic mirror. Each diagnostic line contained an energy meter (Gentec-EO QE25LP) and diagnostic cameras (AVT Manta 145B) to monitor image-relayed beam profiles.

https://doi.org/10.1017/hpl.2023.60 Published online by Cambridge University Press

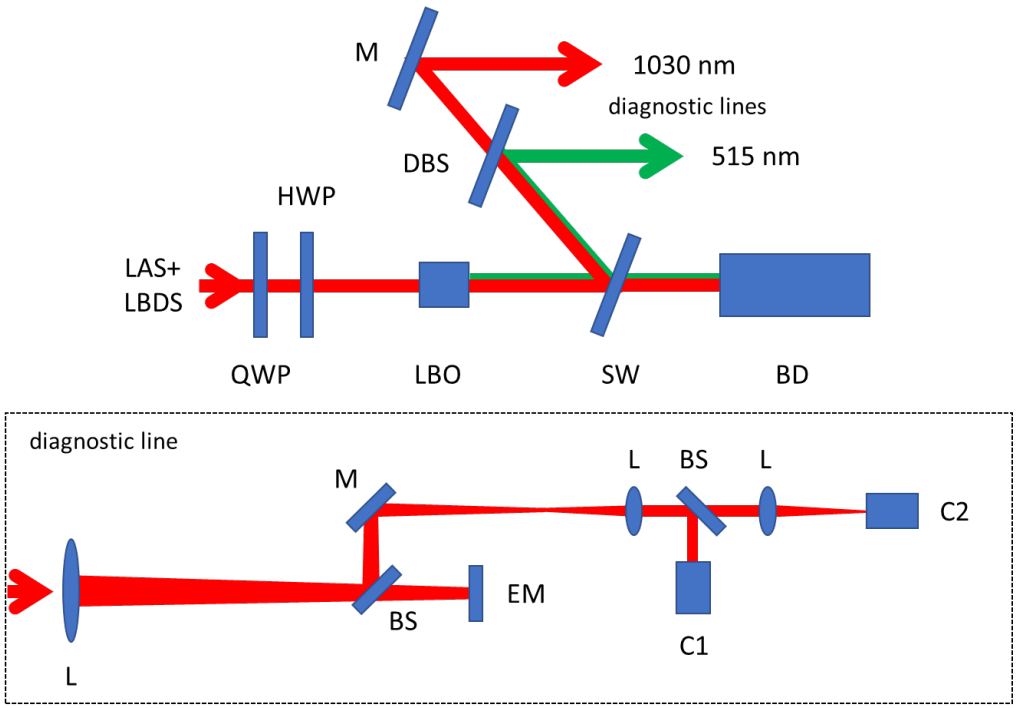

Figure 1 Schematic layout of the conversion experiment. It consists of laser system and laser beam distribution system (LAS+LBDS), quarter waveplate (QWP), half waveplate (HWP), conversion crystal (LBO), partially reflecting sampling wedge (SW) and beam dump (BD). Diagnostics consists of dichroic beamsplitter (DBS), mirrors (M), lenses (L), beamsplitters (BS), energy meter (EM), near field camera (C1) and far field camera (C2). Layout of diagnostic lines is the same for both wavelength and is shown only once.

The laser was operated with output energy of 130 J at repetition rate of 10 Hz. The pulse duration of flat top pulses was 10 ns with rise/fall time of 0.75 ns. The spectrum was centered at 1029.8 nm and bandwidth was around 1 pm. The polarization homogeneity was not uniform across the beam. The main reason for this is the heat dissipated in the amplifier head that generates stresses in the Yb:YAG gain media that create birefringence and change the polarization state of the beam with spatial variability over the beam cross-section. This polarization change is sometimes referred to as depolarization, although this term should be reserved for cases where polarized light is changed into non-polarized. When this beam propagates through a linear polarizer, a portion of its energy is inevitably rejected, and this contributes to energy losses. In the main power amplifier of Bivoj these losses can be as high as 50% (Figure 2 a,b), if linear polarization is used at the amplifier input and without waveplates at the output. We placed a pair of zero order waveplates ($\lambda/2$, $\lambda/4$) after the Faraday isolator after

https://doi.org/10.1017/hpl.2023.60 Published online by Cambridge University Press

the main cryogenic pre-amplifier (10 J) of the Bivoj/DiPOLE system to change input linear polarization into the main cryogenic power amplifier (100 J), the output polarization was adjusted by similar pair in the harmonic conversion setup. By tweaking the input polarization only, the energy losses are decreased to 35% (Figure 2 c,d). If only the output polarization is optimized, the energy losses decrease further to 32% (Figure 2 e,f). By using a custom polarimetric technique to evaluate Mueller matrix of the Bivoj system[11], we were able to estimate numerically the optimal input polarization to further decrease the energy losses to around 3% (Figure 2 g,h). These results were obtained for output energy of 90 J, Helium flow rate of 150 gps and temperature of 120 K. We optimized the polarization homogeneity at lower energy output to avoid changes to the beam as the maximum output energy is close to laser induced damage threshold of optical components. The pump energy was adjusted to operate at the maximum energy extraction from the amplifier. On maximum output energy of 130 J, we used more intense pumping and increased flow rate to 180 gps. We adjusted the polarization homogeneity by slight tweak to all waveplates and the energy losses dropped from around 5% to around 3% with similar profiles as in Figure 2 g,h. Once the polarization homogeneity was optimized, it didn't require any adjustments at the given energy output. Note that vertical polarization is used for SHG.

https://doi.org/10.1017/hpl.2023.60 Published online by Cambridge University Press

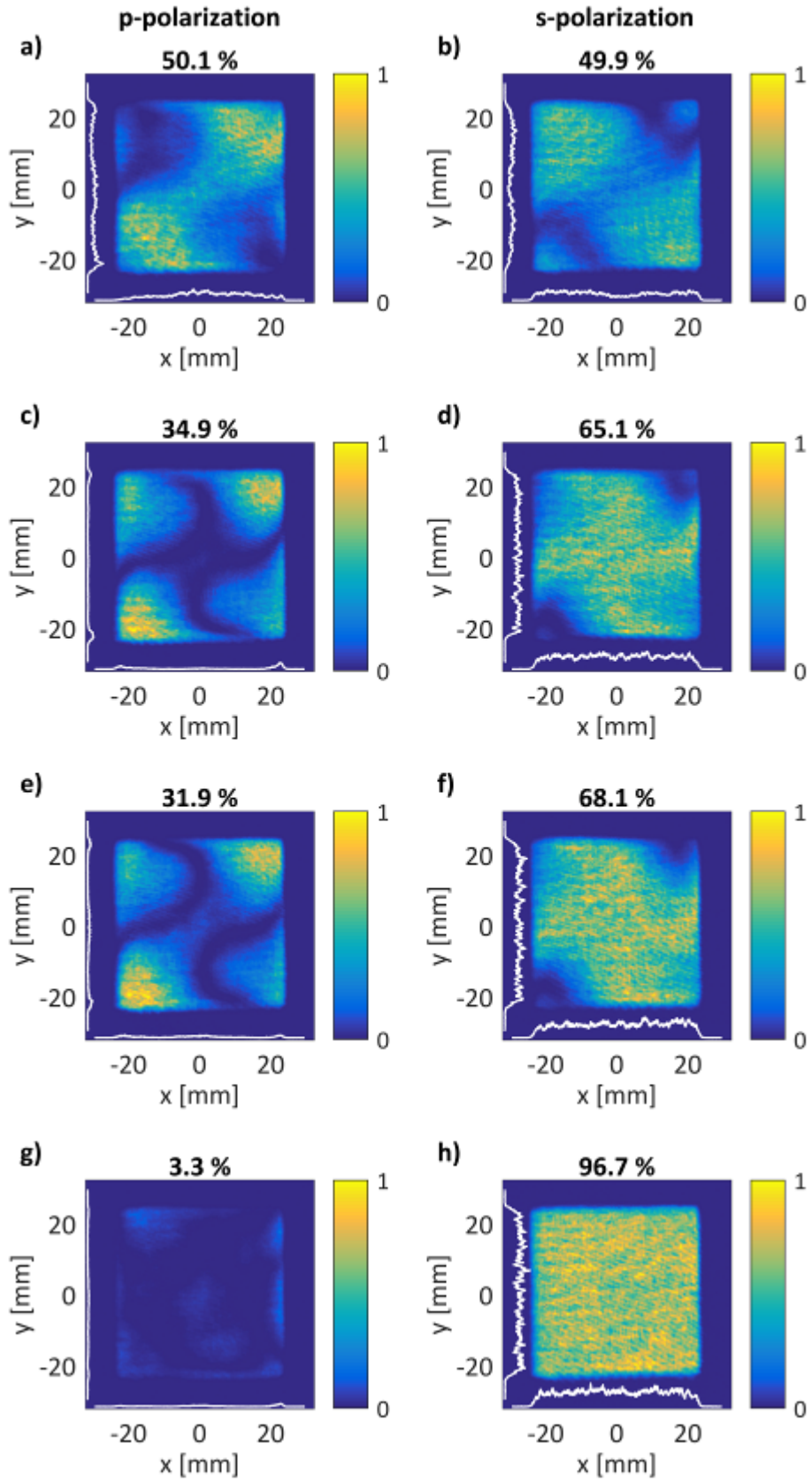

https://doi.org/10.1017/hpl.2023.60 Published online by Cambridge University Press

Figure 2 Beam profiles after correction waveplates after polarizer transmitting vertical polarization (a, c, e, g) or horizonal polarization (b, d, f, h). a, b) for linear polarization entering the power amplifier with no optimization at the output. c, d) for optimized polarization at the input. e, f) for linear polarization at the input and optimized polarization at the output. g, h) for optimized polarization at the input and output. Beam profiles at complementary polarizations were taken under the same conditions and were normalized to sum of both intensities. White lines in the pictures correspond to cross-lines through the center of the beam.

After optimization of polarization homogeneity, the LBO crystal was inserted into the position and aligned using low energy beam. Then the energy was gradually increased up to 130 J at the output of the laser (121 J on the crystal, the transmission of the optics from the output of the laser to LBO crystal was 93.4%) and the phase matching angles were optimized. Energy conversion and conversion efficiency dependence is shown in Figure 3 and its temporal development is shown in Figure 4. The energy of SHG at 515 nm reached the value of 96 J and conversion efficiency of 79%±0.6%. If we would count only the input energy on the polarization that is converted to second harmonic (i.e., neglect the depolarization losses), the conversion efficiency would reach 81.5%±0.6%. Since the oven controls the temperature of the crystal holder, after the beam is propagated through the crystal, the absorption causes the average temperature of the crystal to rise above the set temperature. During this thermalization of the crystal, the converted energy and efficiency dropped, so we re-aligned the phase matching angles several times. While we could compensate for the overall temperature increase in the crystal by adjusting the phase matching angle, the induced temperature gradients could not be compensated in such way. Therefore, the output energy dropped to 94-95 J with conversion efficiency of 76%±0.6%. Converted energy steadily decreased over time, on the order of minutes, but it could be recovered by consecutive phase matching angle optimization. Energy stability of the input beam at fundamental frequency was 0.1% RMS and 0.6% P-t-P (peak-to-peak). Energy stability of the second harmonic beam at the beginning of the experiment was 1.5% RMS and 8% P-t-P (shots 1900-4100) and was caused by rapid heating of the crystal. After thermalization of the crystal

https://doi.org/10.1017/hpl.2023.60 Published online by Cambridge University Press

and re-optimization of the phase matching, the energy stability improved to 0.8% RMS and 6% P-t-P (shots 7500-10000). Further increase in energy stability could be achieved by improving the temperature control of the crystal or automatic phase matching angle optimization, which will be studied in detail in future work. Near field beam profile of the input beam on fundamental frequency and the corresponding converted beam at energy of 95 J is shown in Figure 5 a,b.

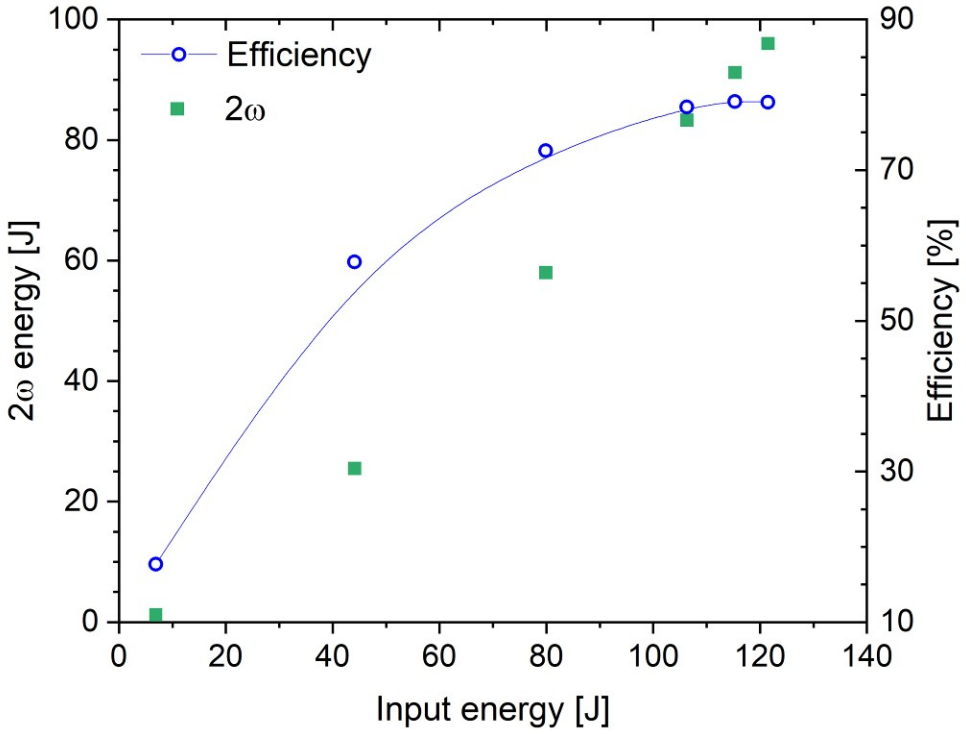

Figure 3 Dependence of second harmonic frequency output energy and conversion efficiency on input energy during the energy ramp in the beginning of the experiment.

https://doi.org/10.1017/hpl.2023.60 Published online by Cambridge University Press

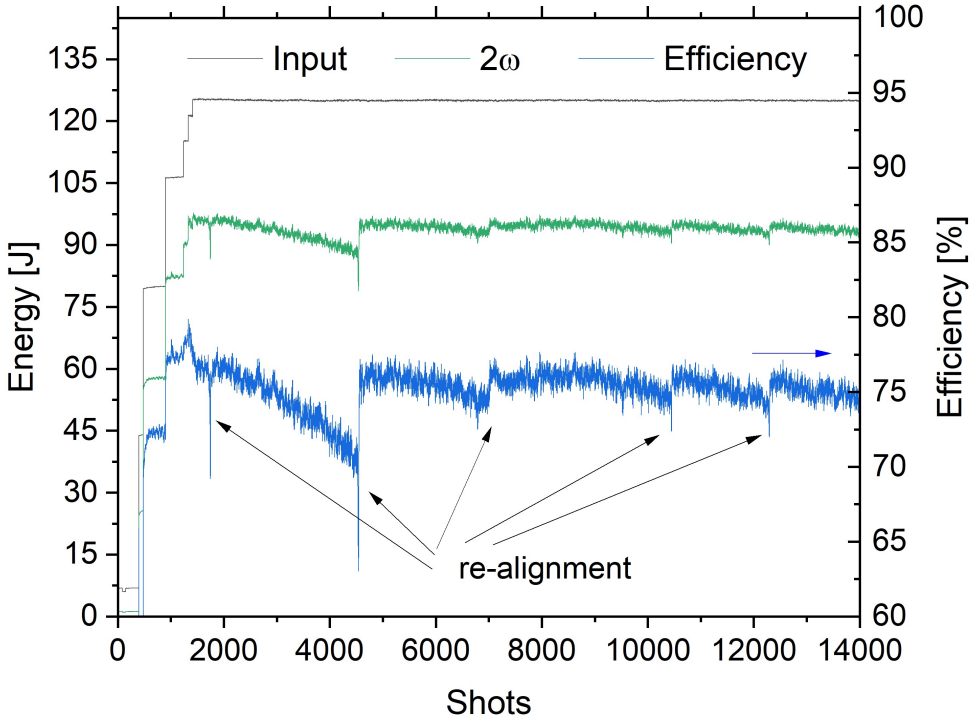

Figure 4 Temporal evolution of the energy of the second harmonic frequency and conversion efficiency. Points where crystal phase matching angle was optimized are marked with arrows.

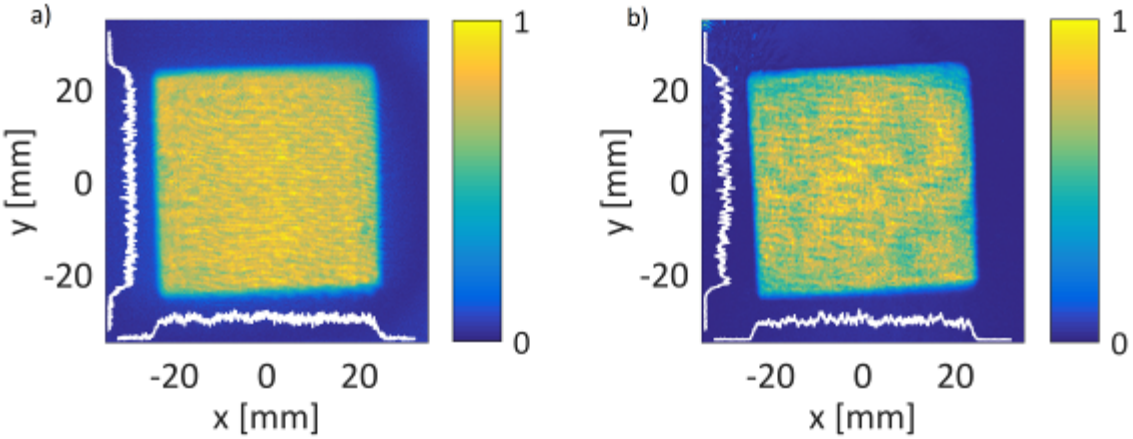

Figure 5 Near field beam profiles of the input beam at 1030 nm with energy of 121 J and converted second harmonic frequency (515 nm) beam with energy of 95 J at the repetition rate of 10 Hz.

III. Conclusion

https://doi.org/10.1017/hpl.2023.60 Published online by Cambridge University Press

The output of SHG of 95 J at 10 Hz at 515 nm was achieved for the first time and represents 58% increase to the state-of-the-art. The second harmonic generation process was achieved using an LBO crystal placed in temperature-controlled holder. The good uniformity of the near field profile of the converted beam and high conversion efficiency has been achieved mainly by addressing the problem of stress induced non-uniform polarization changes originating from within the amplifier chain and their successful mitigation. The reported energy stability of SHG output is on the order of 0.8% RMS, which is below the laser performance capability and is caused mainly by unstable temperature within the LBO crystal due to high average power nature of the working beam. The instability of the crystal temperature will be addressed in the future by optimized design of the temperature stabilization controller.

Correspondence to: Martin Divoky. Email: divoky@fzu.cz

Acknowledgements

European Regional Development Fund and the state budget of the Czech Republic project HiLASE CoE (CZ.02.1.01/0.0/0.0/15_006/0000674); Horizon 2020 Framework Programme (H2020) (739573).

References

1. Sano, Y., Mukai, N., Yoda, M., Uehara, T., Chida, I., and Obata, M., Development and applications of laser peening without coating as a surface enhancement technology, Society of Photo-Optical Instrumentation Engineers (SPIE) Conference Series, vol. 6343, 2006, doi:10.1117/12.707937
2. 7. C. L. Haefner, A. Bayramian, S. Betts, R. Bopp, S. Buck, J. Cupal, M. Drouin, A.

Erlandson, J. Horacek, J. Horner, J. Jarboe, K. Kasl, D. Kim, E. Koh, L. Koubikova, W. Maranville, C. Marshall, D. Mason, J. Menapace, P. Miller, P. Mazurek, A. Naylon, J. Novak, D. Peceli, P. Rosso, K. Schaffers, E. Sistrunk, D. Smith, T. Spinka, J. Stanley, R. Steele, C. Stolz, T. Suratwala, S. Telford, J. Thoma, D. VanBlarcom, J. Weiss, P. Wegner, "High average power, diode pumped petawatt laser systems: a new generation of lasers enabling precision science and commercial applications", *Proceedings of SPIE 10241*, 1024102-1-5 (SPIE Optics + Optoelectronics, 2017, Prague, Czech Republic)

3. https://www.clf.stfc.ac.uk/Pages/EPAC-introduction-page.aspx
4. G. Archipovaite, M. Galletti, P. Oliveira, M. Ahmad, R. Clarke, D. Neely, N. Booth, R. Heathcote, M. Galimberti, I. Musgrave, and C. Hernandez-Gomez, "Progress of the development of new Vulcan PW OPCPA beamline", in *in 2019 Conference on Lasers and Electro-Optics Europe and European Quantum Electronics Conference,* OSA Technical Digest (Optica Publishing Group, 2019), paper ca_2_2
5. https://www.llnl.gov/news/national-ignition-facility-achieves-fusion-ignition , 22.12.2022
6. Röcker, C., Loescher, A., Bienert, F., Villeval, P., Lupinski, D., Bauer, D., Killi, A., Graf, T., and Abdou Ahmed, M., Ultrafast green thin-disk laser exceeding 1.4 kW of average power, Optics Letters, vol. 45, 2020, doi:10.1364/OL.403781
7. Chi, H., Wang, Y., Davenport, A., Menoni, C.S., and Rocca, J.J., Demonstration of a kilowatt average power, 1 J, green laser, Optics Letters, vol. 45, 2020, doi:10.1364/OL.412975
8. Phillips, J.P., Banerjee, S., Mason, P., Smith, J., Spear, J., De Vido, M., Ertel, K., Butcher, T., Quinn, G., Clarke, D., Edwards, C., Hernandez-Gomez, C., and Collier, J., Second and third harmonic conversion of a kilowatt average power, 100-J-level diode pumped

https://doi.org/10.1017/hpl.2023.60 Published online by Cambridge University Press

Yb:YAG laser in large aperture LBO, Optics Letters, vol. 46, 2021, doi:10.1364/OL.419861

9. Mason, P., Divoký, M., Ertel, K., Pilař, J., Butcher, T., Hanuš, M., Banerjee, S., Phillips, J., Smith, J., De Vido, M., Lucianetti, A., Hernandez-Gomez, C., Edwards, C., Mocek, T., and Collier, J., Kilowatt average power 100 J-level diode pumped solid state laser, Optica, vol. 4, 2017, doi:10.1364/OPTICA.4.000438
10. Divoký, M., Pilař, J., Hanuš, M., Navrátil, P., Denk, O., Severová, P., Mason, P., Butcher, T., Banerjee, S., De Vido, M., Edwards, C., Collier, J., Smrž, M., and Mocek, T., 150 J DPSSL operating at 1.5 kW level, Optics Letters, vol. 46, 2021, doi:10.1364/OL.444902
11. Slezák, O., Sawicka-Chyla, M., Divoký, M., Pilař, J., Smrž, M., and Mocek, T., Thermal-stress-induced birefringence management of complex laser systems by means of polarimetry, Scientific Reports, vol. 12, 2022, doi:10.1038/s41598-022-22698-9

Figures and tables

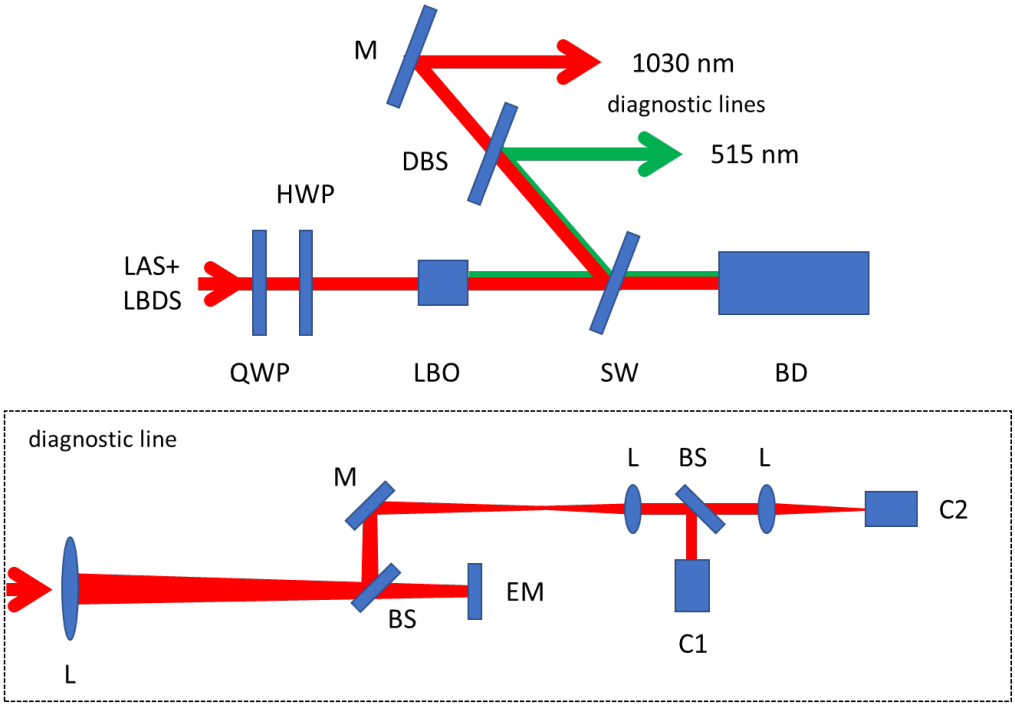

https://doi.org/10.1017/hpl.2023.60 Published online by Cambridge University Press

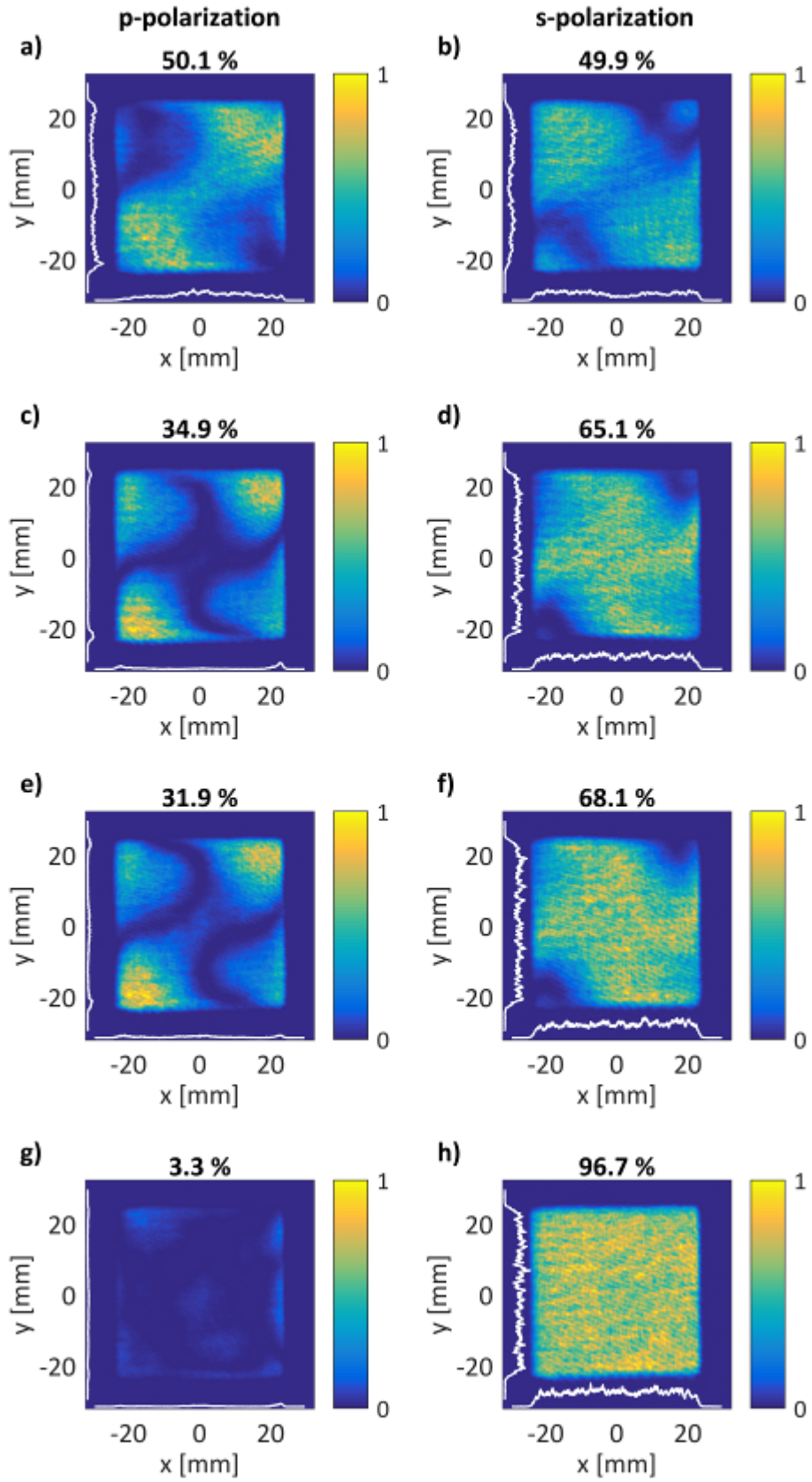

https://doi.org/10.1017/hpl.2023.60 Published online by Cambridge University Press

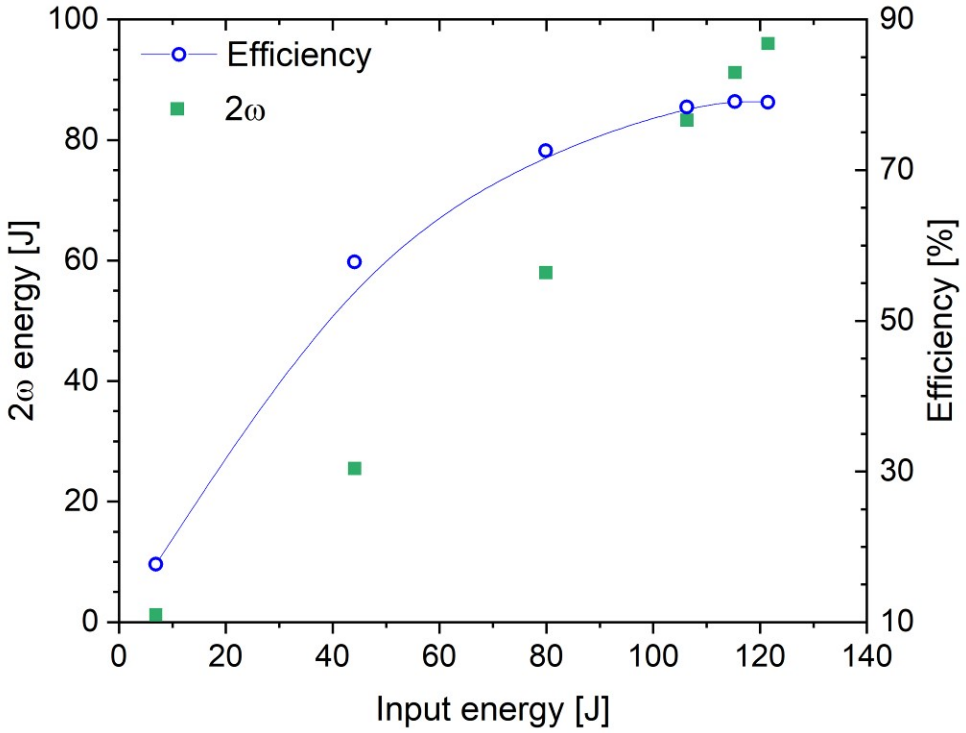

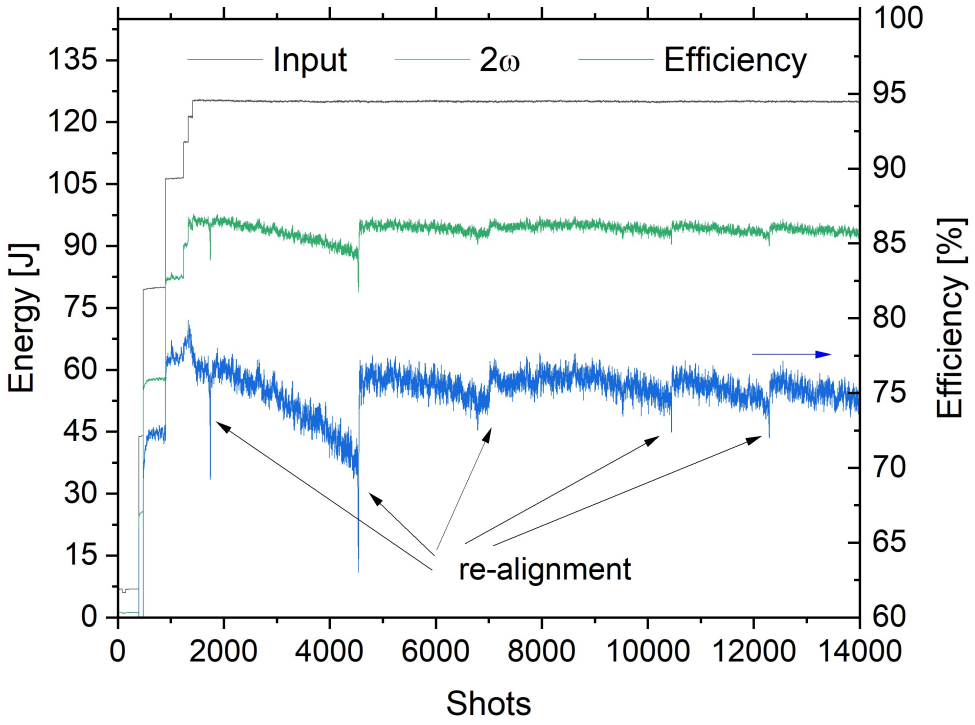

https://doi.org/10.1017/hpl.2023.60 Published online by Cambridge University Press

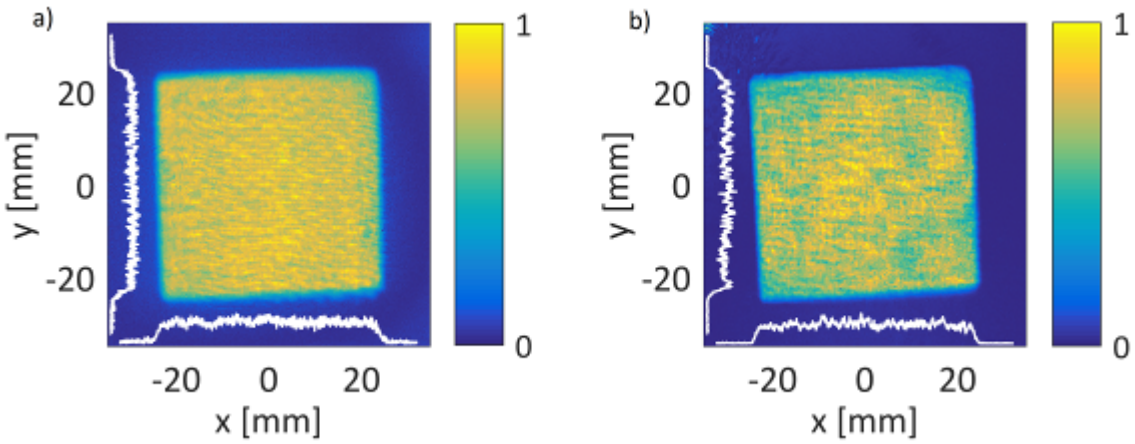

Figure and table captions

Figure 6 Schematic layout of the conversion experiment. It consists of laser system and laser beam distribution system (LAS+LBDS), quarter waveplate (QWP), half waveplate (HWP), conversion crystal (LBO), partially reflecting sampling wedge (SW) and beam dump (BD). Diagnostics consists of dichroic beamsplitter (DBS), mirrors (M), lenses (L), beamsplitters (BS), energy meter (EM), near field camera (C1) and far field camera (C2). Layout of diagnostic lines is the same for both wavelength and is shown only once.

Figure 7 Beam profiles after correction waveplates after polarizer transmitting vertical polarization (a, c, e, g) or horizonal polarization (b, d, f, h). a, b) for linear polarization entering the power amplifier with no optimization at the output. c, d) for optimized polarization at the input. e, f) for linear polarization at the input and optimized polarization at the output. g, h) for optimized polarization at the input and output. Beam profiles at complementary polarizations were taken under the same conditions and were normalized to sum of both intensities. White lines in the pictures correspond to cross-lines through the center of the beam.

Figure 8 Dependence of second harmonic frequency output energy and conversion efficiency on input energy during the energy ramp in the beginning of the experiment.

Figure 9 Temporal evolution of the energy of the second harmonic frequency and conversion efficiency. Points where crystal phase matching angle was optimized are marked with arrows.

Figure 10 Near field beam profiles of the input beam at 1030 nm with energy of 121 J and converted second harmonic frequency (515 nm) beam with energy of 95 J at the repetition rate of 10 Hz.

https://doi.org/10.1017/hpl.2023.60 Published online by Cambridge University Press